SUPPORTING INFORMATION (SI) APPENDIX

Metabolic Features of Chronic Fatigue Syndrome

Naviaux RK, *et al.,* 2016

SI RESULTS

Fatty Acid and Endocannabinoid Metabolism was Disturbed in Females

Plasma adipoylcarnitine is a six-carbon dicarboxylic acid (C6DC) carnitine ester that was increased in females with chronic fatigue syndrome, but not in males (Table 2AB). Elevations in adipoylcarnitine are sensitive indicator of decrease in riboflavin dependent mitochondrial beta oxidation of fatty acids(1), and fasting(2). Fasting, or decreased intracellular allocation of fatty acids for oxidation in mitochondria results in the induction of the peroxisomal enzyme known as the NAD+ activated, L-bifunctional enzyme (enoyl-CoA, hydratase/3-hydroxyacyl CoA dehydrogenase, EHHADH). This enzyme is required for the synthesis of medium chain dicarboxylic acids like adipic acid(3). Spurious elevations of adipoylcarnitine can be seen as the result of high volume consumption of adipic acid-containing jello or gelatin(4), but this is not a viable explanation in this study.

Plasma 2-arachidinoyl glycerol (2AG) was decreased in females with CFS, but not in males (Table 2AB). 2AG is a natural cannabinoid agonist of CB1 signaling. Inhibition of CB1 receptors is known to inhibit fatty acid oxidation and increase plasma levels of adipoyl carnitine(5). The observed decrease in 2AG might contribute to decreased oxidation of adipic acid and increased plasma adipoylcarnitine.

Plasma 2-octenoylcarnitine is an eight-carbon mono-unsaturated fatty acid (C8:1) carnitine ester that was decreased in females with chronic fatigue syndrome, but not in males (Tables 2AB). Elevations of octenoylcarnitine are seen in calorie excess conditions such as obesity and metabolic syndrome(6). Decreased octenoic acid is also known to inhibit the susceptibility to

Herpes virus infections and to increase cell membrane stiffness(7). Octenoic acid is produced as an intermediate of mitochondrial fatty acid and lipoic acid synthesis(8). It is the substrate for mitochondrial enoyl thioester reductase (ETR), a family of enzymes that requires NADPH to reduce the double bond to octanoic acid, which is then used for lipoic acid synthesis(8). Decreased levels of this C8:1 acylcarnitine are consistent with decreased mitochondrial fatty acid synthesis, increased oxidation, increased renal secretion, or a combination of the three. All other acylcarnitine species measured (C2-24) were normal in both males and females. No abnormalities of fatty acid oxidation were found in males with chronic fatigue syndrome.

Serine and Threonine were Increased in Males

Plasma serine and threonine levels were increased in males with chronic fatigue syndrome, but not in females (Table 2AB). The intracellular ratio of serine to glycine is a key regulator of 1-carbon, nucleotide, and folate metabolism(9). L-Serine is also an essential precursor of sphingolipid, phosphatidylserine, D-serine, and *de novo* cysteine and glutathioine synthesis. Both serine and threonine are gluconeogenic amino acids that can be used to make glucose during fasting or stress. Acute stress or infection results in a decrease in both plasma serine and threonine levels(10, 11). An increase in these amino acids is consistent with increased synthesis, decreased utilization, decreased renal excretion, or a combination of all three in males with chronic fatigue syndrome. With regards to decreased utilization, the sharply reduced levels of sphingolipids that require serine for synthesis, would contribute to a serine sparing.

Sphingolipids and Glycosphingolipids were Decreased

Increased sphingolipids are a recently recognized hallmark of obesity(12), metabolic syndrome, insulin resistance(13), and a risk factor in Alzheimer dementia(14). These abnormalities are improved by exercise(15), and caloric restriction(16). Effective methods to increase abnormally low sphingolipids have not yet been developed.

Cholesterol Synthesis through the Lathosterol Pathway was Decreased

The final conversion of desmosterol to cholesterol is catalyzed by the FAD-, and NADPH-requiring enzyme, 24-dehydrocholesterol reductase (DHCR24)(17, 18). When DHCR24 is downregulated, desmosterol accumulates in cell membranes, but does not change significantly in plasma. Membrane accumulation of desmosterol inhibits endocytosis and pinocytotic import through caveolae, and inhibiting the production of sphingolipid-rich and cholesterol-rich lipid rafts needed for cell-cell signaling(18). This would serve as a cell defense mechanism that inhibits the uptake of certain intracellular bacterial pathogens as Coxiella (Q fever)(19) and Borrelia (Lyme disease)(20, 21).

Chronic Fatigue Syndrome Patients had an Average of 40 Metabolic Abnormalities

The mean number of metabolites falling outside of the 95% confidence limits (beyond 2 standard deviations from the mean) in females with chronic fatigue patients was 40 (+/- 3.5) (mean +/- SEM; Figure 1E), and 41 (+/- 4.4) in males (SI Figure S2A). This was significantly more than the number found among age and sex-matched controls, which was 16 (+/- 1.8) ($p < 2 \times 10^{-6}$; SI Figure S2A). The mean and 95% confidence interval for the number of abnormalities expected by chance in the controls was calculated from the binomial distribution of 420 measured metabolites with a mean chance of abnormality equal to the p value of 0.05 for each test. The total number of abnormalities expected in controls was 21, with a range of 13-32 (95% CI = 13-32; 420 x 0.05 = 21). The metabolites that were altered most in chronic fatigue syndrome were ranked by multivariate analysis (SI Figure S3AB). Individual metabolite abnormalities were visualized according to a conventional biochemical pathway wall chart-style organization created in Cytoscape (SI Figure A4AB). Metabolites that were decreased were colored green and those that were increased in chronic fatigue were colored red.

Mass Spectrometry and Metabolomics Quality Control

Data from a representative quality control series are reported in SI Tables S2 and S3. The within-day Pearson correlation of 27 internal stable-isotope labeled standards and 50 endogenous unlabeled metabolites was 0.999 and 0.998, respectively (SI Table S2). The total variation associated with replicate sample processing was found to be 9-11% (SI Table S2).

We next quantified the reproducibility of 420-460 targeted metabolites by running two representative plasma samples in triplicate on three sequential days. A total of 458 metabolite AUCs in two plasma samples were quantified in the series illustrated. The Pearson correlation r values were 0.983 in one sample and 0.981 in another. The median of the relative standard deviations (RSD) from 458 metabolites measured in triplicate on 3 days was 12.1%-12.5% (SI Table S3).

SI DISCUSSION

Sphingolipids, Chronic Fatigue, and Dauer

Depletion of plasma sphingolipids and glycosphingolipids explained 55% of the metabolic disturbances in males and 44% in females with chronic fatigue syndrome (Table 2AB). All sphingolipids are synthesized from the amino acid serine and palmitoyl-CoA(22). Ceramides are produced rapidly from sphingomyelins by the inducible enzyme acid sphingomyelinase (ASMase)(23) and redox regulated neutral sphingomyelinase (nSMase)(24). Ceramides, and gangliosides made from ceramides, are important components of cell membrane patches and microdomains called lipid rafts that mobilize and aggregate during cell activation or infection. Sphingolipid rafts are enriched in cholesterol, and are crucial for cell-cell signaling, and reactive oxygen species (ROS) production for oxidative shielding(25) and defense(26). Ceramide-, ganglioside-, and cholesterol-enriched cell membrane rafts are needed to recruit protein receptor and effector subunits during cell activation(27), cardiovascular(28) and renal(29)

disease, and bacterial(30) and protozoal(31) infections. Increased membrane expression and release of sphingolipids is a universal response to acute infection, but can also be hijacked as a vehicle for virus entry and spread(32), and can result in autoimmune responses to gangliosides(33), and to lipid raft-associated receptors like CD46(34). Down-regulation of sphingolipids in chronic fatigue syndrome is consistent with a compensatory response to environmental stress, inflammation, or infection. Down-regulation of sphingolipid synthesis in general, and ceramide synthesis specifically, decreases the risk of apoptosis in response to new viral or bacterial infections(26), and is a feature of dauer(35). Mechanistic studies of the path by which the hypometabolic state is normally exited after viral illness, or in model systems after dauer may provide insights that will be useful in treating patients with chronic fatigue syndrome.

SI MATERIALS AND METHODS

Sample Collection

Venous blood was collected between the hours of 8 am and 5 pm, at least 3 hours after the last meal, into lithium-heparin vacutainer tubes (BD #367884). Plasma was separated by centrifugation at 900g x 10 minutes at room temperature within one hour of collection. The resulting fresh lithium-heparin plasma was transferred to labeled 1.2 ml or 2.0 ml externally threaded, cryotubes with a minimum headspace air gap for storage at -80˚C for analysis.

Metabolomics

Samples were analyzed on an AB SCIEX QTRAP 5500 triple quadrupole mass spectrometer equipped with a Turbo V electrospray ionization (ESI) source, Shimadzu LC-20A UHPLC system, and a PAL CTC autosampler. Typically, 90 µl of plasma was thawed on ice and transferred to a 1.7 ml Eppendorf tube. Five (5.0) µl of a cocktail containing 25-35 commercial stable isotope internal standards, and 5.0 µl of 57 stable isotope internal standards that were custom-synthesized in *E. coli* and *S. cerevisiae* by metabolic labeling with ^{13}C-glucose and ^{13}C-

bicarbonate, were added, mixed, and incubated for 10 min at 20˚C to permit small molecules and vitamins in the internal standards to associate with plasma binding proteins. Macromolecules (protein, DNA, RNA, glycans, etc.) were precipitated by extraction with 4 volumes (400 µl) of cold (-20˚C), acetonitrile:methanol (50:50) (LCMS grade, Cat# LC015-2.5 and GC230-4, Burdick & Jackson, Honeywell), vortexed vigorously, and incubated on crushed ice for 10 min, then removed by centrifugation at 16,000g x 10 min at 4˚C. The supernatants containing the extracted metabolites and internal standards in the resulting 40:40:20 solvent mix of acetonitrile:methanol:water were transferred to labeled cryotubes and stored at -80˚C for LC-MS/MS analysis.

LC-MS/MS analysis was performed by scheduled multiple reaction monitoring (sMRM) under Analyst v1.6.2 software control in both negative and positive mode with rapid polarity switching (50 ms). Nitrogen was used for curtain gas (set to 30), collision gas (set to high), ion source gas 1 and 2 (set to 35). The source temperature was 500˚C. Spray voltage was set to -4500 V in negative mode and 5500 V in positive mode. The values for Q1 and Q3 mass-to-charge ratios (m/*z*), declustering potential (DP), entrance potential (EP), collision energy (CE), and collision cell exit potential (CXP) were determined and optimized for each MRM for each metabolite. Ten microliters of extract was injected by PAL CTC autosampler via a 10 µl stainless steel loop into a 250 mm × 2.0 mm, 4µm polymer based NH2 HPLC column (Asahipak NH2P-40 2E, Showa Denko America, Inc., NY) held at 25°C for chromatographic separation. The mobile phase was solvent A: 95% water with 20 mM $(NH_4)_2CO_3$ (Sigma, Fluka Cat# 74415-250G-F), 5% acetonitrile, and 38 mM NH_4OH (Sigma, Fluka Cat# 17837-100ML), final pH 9.75; solvent B: 100% acetonitrile. Separation was achieved using the following gradient: 0-3.5 min: 95%B, 3.6-8 min: 85% B, 8.1-13 min: 75% B, 13.5–35 min: 0% B, 36–46 min: 95% B, 46.1 min: end. The flow rate was 200 µl/min. Pump pressures ranged from 920-2600 psi over the course of the gradient. All the samples were kept at 4°C during analysis. The chromatographic peaks were

identified using MultiQuant (v3, AB Sciex), confirmed by manual inspection, and the peak areas integrated.

Metabolomics Quality Control

We routinely quantified two levels of reproducibility before passing metabolomic results for data analysis. In the first level, we quantified the variability introduced by pipetting of stable-isotope labeled internal standards and sample extraction efficiency. We referred to this as the work-flow quality control. Starting from a standardized lot of pooled human plasma, we divided this into 3 samples. Stable isotope-labeled internal standards (SIL-ISDs) were added to each sample and extracted. Each extract was then injected 3 times each day for 3 days. Measurements of 27 stable isotope-labeled standards and 50 endogenous metabolites were monitored daily for process control. Reproducibility was quantified by calculating the within day, and within plus between day Pearson correlations, and median of the relative standard deviations (RSD) (SI Table S2). In the second level of quality control we quantified the metabolite areas under the curve (AUCs) of 420 to 460 targeted molecules by scheduled Multiple Reaction Monitoring (sMRM) using at least 2 mass transitions per molecule, in 2 representative plasma samples injected in triplicate on 3 days (SI Table S3).

Metabolic Pathway Visualization in Cytoscape

We constructed a rendering of mammalian intermediary metabolism in Cytoscape v 3.1.1 (http://www.cytoscape.org/). Pathways represented in the network for Chronic Fatigue Syndrome included the 20 metabolic pathways associated with the cell danger response(36) that were dysregulated. Nodes in the Cytoscape network represent metabolites within the pathways and have been colored according to the Z-score. The Z-score was computed as the arithmetic difference between the mean concentration of each metabolite in Chronic Fatigue and controls, divided by the standard deviation in the controls. Node colors were arranged on a

red-green color scale with green representing ≤-2.00 Z-score, red representing ≥+2.00 Z-score, and with a zero (0) Z-score represented as white. The sum of the VIP scores from metabolites with VIP scores >1.5 for each metabolic pathway was displayed percentage of total biochemical impact next to the pathway name.

SI REFERENCES

1. Bates CJ (1989) Metabolism of [14C]adipic acid in riboflavin-deficient rats: a test in vivo for fatty acid oxidation. *The Journal of nutrition* 119(6):887-891.
2. Tserng KY, Griffin RL, & Kerr DS (1996) Distinction of dicarboxylic aciduria due to medium-chain triglyceride feeding from that due to abnormal fatty acid oxidation and fasting in children. *Metabolism* 45(2):162-167.
3. Houten SM*, et al.* (2012) Peroxisomal L-bifunctional enzyme (Ehhadh) is essential for the production of medium-chain dicarboxylic acids. *Journal of lipid research* 53(7):1296-1303.
4. Glick N & Fischer M (1991) Adipic aciduria, a dietary artefact. *Journal of inherited metabolic disease* 14(5):849-850.
5. Tomlinson L*, et al.* (2012) Cannabinoid receptor antagonist-induced striated muscle toxicity and ethylmalonic-adipic aciduria in beagle dogs. *Toxicological sciences : an official journal of the Society of Toxicology* 129(2):268-279.
6. Mai M*, et al.* (2013) Serum levels of acylcarnitines are altered in prediabetic conditions. *PloS one* 8(12):e82459.
7. Galdiero F, Folgore A, Galdiero M, & Tufano MA (1990) Effect of modification of HEp 2 cell membrane lipidic phase on susceptibility to infection from herpes simplex virus. *Infection* 18(6):372-375.
8. Hiltunen JK, Chen Z, Haapalainen AM, Wierenga RK, & Kastaniotis AJ (2010) Mitochondrial fatty acid synthesis--an adopted set of enzymes making a pathway of major importance for the cellular metabolism. *Prog Lipid Res* 49(1):27-45.
9. Naviaux RK (2008) Mitochondrial control of epigenetics. *Cancer biology & therapy* 7(8):1191-1193.
10. Komarov AM & Reddy MN (1998) Effect of septic shock on nitrate, free amino acids, and urea in murine plasma and urine. *Clin Biochem* 31(2):107-111.
11. Faure M*, et al.* (2007) Threonine utilization for synthesis of acute phase proteins, intestinal proteins, and mucins is increased during sepsis in rats. *The Journal of nutrition* 137(7):1802-1807.
12. Hanamatsu H*, et al.* (2014) Altered levels of serum sphingomyelin and ceramide containing distinct acyl chains in young obese adults. *Nutr Diabetes* 4:e141.
13. Chavez JA & Summers SA (2012) A ceramide-centric view of insulin resistance. *Cell metabolism* 15(5):585-594.
14. van Echten-Deckert G & Walter J (2012) Sphingolipids: critical players in Alzheimer's disease. *Prog Lipid Res* 51(4):378-393.
15. Bergman BC*, et al.* (2015) Serum sphingolipids: relationships to insulin sensitivity and changes with exercise in humans. *American journal of physiology. Endocrinology and metabolism* 309(4):E398-408.
16. Hernandez-Corbacho MJ*, et al.* (2011) Accumulation of long-chain glycosphingolipids during aging is prevented by caloric restriction. *PloS one* 6(6):e20411.
17. Spann NJ*, et al.* (2012) Regulated accumulation of desmosterol integrates macrophage lipid metabolism and inflammatory responses. *Cell* 151(1):138-152.
18. Zerenturk EJ, Sharpe LJ, Ikonen E, & Brown AJ (2013) Desmosterol and DHCR24: unexpected new directions for a terminal step in cholesterol synthesis. *Prog Lipid Res* 52(4):666-680.
19. Gilk SD*, et al.* (2013) Bacterial colonization of host cells in the absence of cholesterol. *PLoS Pathog* 9(1):e1003107.

20. LaRocca TJ*, et al.* (2013) Proving lipid rafts exist: membrane domains in the prokaryote Borrelia burgdorferi have the same properties as eukaryotic lipid rafts. *PLoS Pathog* 9(5):e1003353.
21. Toledo A, Monzon JD, Coleman JL, Garcia-Monco JC, & Benach JL (2015) Hypercholesterolemia and ApoE deficiency result in severe infection with Lyme disease and relapsing-fever Borrelia. *Proceedings of the National Academy of Sciences of the United States of America* 112(17):5491-5496.
22. Wennekes T*, et al.* (2009) Glycosphingolipids--nature, function, and pharmacological modulation. *Angew Chem Int Ed Engl* 48(47):8848-8869.
23. Seitz AP, Grassme H, Edwards MJ, Pewzner-Jung Y, & Gulbins E (2015) Ceramide and sphingosine in pulmonary infections. *Biol Chem* 396(6-7):611-620.
24. Dotson PP, 2nd, Karakashian AA, & Nikolova-Karakashian MN (2015) Neutral sphingomyelinase-2 is a redox sensitive enzyme: role of catalytic cysteine residues in regulation of enzymatic activity through changes in oligomeric state. *The Biochemical journal* 465(3):371-382.
25. Naviaux RK (2012) Oxidative shielding or oxidative stress? *J Pharmacol Exp Ther* 342(3):608-618.
26. Becker KA, Gellhaus A, Winterhager E, & Gulbins E (2008) Ceramide-enriched membrane domains in infectious biology and development. *Subcell Biochem* 49:523-538.
27. Jin S, Zhou F, Katirai F, & Li PL (2011) Lipid raft redox signaling: molecular mechanisms in health and disease. *Antioxidants & redox signaling* 15(4):1043-1083.
28. Li X, Becker KA, & Zhang Y (2010) Ceramide in redox signaling and cardiovascular diseases. *Cell Physiol Biochem* 26(1):41-48.
29. Li PL & Zhang Y (2013) Cross talk between ceramide and redox signaling: implications for endothelial dysfunction and renal disease. *Handbook of experimental pharmacology* (216):171-197.
30. Grassme H*, et al.* (2003) Host defense against Pseudomonas aeruginosa requires ceramide-rich membrane rafts. *Nat Med* 9(3):322-330.
31. Chowdhury KD, Sen G, Sarkar A, & Biswas T (2011) Role of endothelial dysfunction in modulating the plasma redox homeostasis in visceral leishmaniasis. *Biochimica et biophysica acta* 1810(7):652-665.
32. Schneider-Schaulies J & Schneider-Schaulies S (2013) Viral infections and sphingolipids. *Handbook of experimental pharmacology* (216):321-340.
33. Wakerley BR & Yuki N (2013) Infectious and noninfectious triggers in Guillain-Barre syndrome. *Expert review of clinical immunology* 9(7):627-639.
34. Persson BD*, et al.* (2010) Structure of the extracellular portion of CD46 provides insights into its interactions with complement proteins and pathogens. *PLoS Pathog* 6(9):e1001122.
35. Cutler RG, Thompson KW, Camandola S, Mack KT, & Mattson MP (2014) Sphingolipid metabolism regulates development and lifespan in Caenorhabditis elegans. *Mechanisms of ageing and development* 143-144:9-18.
36. Naviaux RK (2014) Metabolic features of the cell danger response. *Mitochondrion* 16:7-17.

SI FIGURE LEGENDS

1. **Figure S1. Geographical Distribution of Chronic Fatigue Syndrome Cases and Controls.** Patients and controls were recruited from 51 zip codes around the US and Canada. Most subjects were residents of California. Cases are indicated in red. Controls in blue.
2. **Figure S2. Characterization of total, low, and high metabolite abnormalities in chronic fatigue syndrome.** A. Males, B. Females. Metabolites with Z-scores ≥ 2.0 are indicated in red. Metabolites with Z-scores ≤ -2.0 are indicated in green. Both the total number of metabolite abnormalities and the number of metabolites that were decreased were significantly increased in patients with chronic fatigue syndrome.
3. **Figure S3. Rank Order of Distinguishing Metabolite Abnormalities in Chronic Fatigue Syndrome. A. Males, B. Females.** Partial least squares discriminant analysis (PLSDA) was used to rank the most significantly abnormal metabolites by variable importance in projection (VIP) scores. VIP scores ≥ 1.5 were considered significant. The top 35 most dysregulated metabolites are illustrated. See supplemental online material Table S1 for a complete listing of all 61 metabolites with VIP scores ≥ 1.5.
4. **Figure S4. Cytoscape visualization of metabolite and pathway disturbances in chronic fatigue syndrome. A. Males, B. Females.** The fractional contribution of each pathway is indicated as a percentage of the total variable importance in projection (VIP) score in black circles. The smaller circles indicate the measured metabolites in each pathway, quantified by z-score. Metabolites in red were increased and those in green were decreased in chronic fatigue syndrome compared to controls.
5. **Figure S5. The distribution of diagnostic and personalized metabolic abnormalities in chronic fatigue syndrome, Males.** The number of abnormal metabolites that were diagnostic for chronic fatigue syndrome, as determined by multivariate analysis, is indicated

in green. The number of metabolites that are abnormal (≥ 2 standard deviations above or below the control mean), but are not specifically characteristic of CFS is indicated in red. The graph for females is shown in Figure 1F.

6. **Figure S6. Mitochondrial Control of Redox, NADPH, Nucleotide, and Methylation Pathways.** In embryonic cells and cancer, MTHFD2L is expressed and one-carbon units are efficiently converted to Formyl-THF and formate for cytosolic nucleotide synthesis. Under these conditions, fewer one-carbon units are available for SAM synthesis and DNA methylation. When MTHFD2L is turned down in differentiated cells, less mitochondrial formate is produced and one-carbon units are directed through Methylene-THF toward increased SAM synthesis and increased DNA methylation. 1/2--Mitochondrial Bifunctional Enzyme (mBE, MTHFD2L): 1--NAD(P)+ Dependent Methylene Tetrahydrofolate Reductase, 2--Methenyl-THF Cyclohydrolase. 3--Formyl-THF Synthase (FTS), 3*--FTS can reverse directions in differentiated cells when MTHFD2L is decreased, 4--Mitochondrial Serine Hydroxymethyl Transferase (mSHMT), 5--Dimethylglycine Dehydrogenase, ETF--Electron Transfer Flavoprotein, 6--Sarcosine Dehydrogenase, 7--Glycine Cleavage System, 8--Methylene-THF Reductase (MTFR). 9--Thymidylate Synthase, 10--Dihydrofolate Reductase (DHFR). 11--Cytosolic Serine Hydroxymethyl Transferase (cSHMT). 11*--cSHMT reverse reaction, 12/13/14--Cytosolic Trifunctional Enzyme (cTE): 12/13/14--Cytosolic Trifunctional C1-THF Synthase (MTHFD1) [12--Formyl-THF Synthase, 13--Methenyl-THF Cyclohydrolase, 14--NADPH-dependent Methylene-THF Dehydrogenase], 15--Formyl-THF Dehydrogenase, 16--Homocysteine Methyl Transferase (Methionine Synthase, CblG). 17--Methionine Adenosyl Transferase (MAT). 18*--Multiple DNA-, RNA-, Protein--, Neurotransmitter, and Other Methyltransferase reactions in the nucleus, cytosol, and mitochondria. 19--S-Adenosyl Homocysteine Hydrolase (SAHH), 20--Cystathionine β-Synthase (CBS), 21—Cystathionase (Cystathionine γ-lyase), 22--γ-Glutamylcysteine Synthase (GCS), 23--

Glutathione Synthase, 24--Nucleoside Diphosphate Kinase, 25--ATP Synthase (Complex V), 26--Propionyl CoA Carboxylase, 27--Methylmalonyl CoA Mutase, 28--Betaine Homocysteine Methyltransferase, 29--Choline Dehydrogenase, 30--Betaine Aldehyde Dehydrogenase, 31--S-Adenosylmethionine decarboxylase (adoMetDC, AMD1, SAMDC), 32--Spermidine synthase, 33--Spermine synthase, 34--Methylthioadenosine phosphorylase (MTAP), 35--Methionine synthase reductase (MSR, MTRR, CblE), 36--Delta Amino Levulinic Acid Synthase (dALAS), 37--Glutathione reductase, GAR--Glycinamide Ribonucleotide, AICAR--Aminoimidazole Carboxamide Ribonucleotide, FAICAR--Formaminoimidazole Carboxamide Ribonucleotide, Ado--Adenosine, NAC--N-Acetyl Cysteine, dcSAM--Decarboxylated S-Adenosyl Methionine, MTA--Methylthioadenosine, MTR-1P--Methylthioribose 1-phosphate, B6 (Pyridoxine, Pyridoxal phosphate, PLP), FAD--Flavin adenine dinucleotide, FMN--Flavin mononucleotide, GSH--reduced glutathione, GSSG--oxidized glutathione disulfide. A less detailed version of this figure was published by Dr. Naviaux in 2008(9).

7. **Figure S7. Principal Components Analysis (PCA). A. Males, B. Females.** Scree plots illustrate the cumulative (green line) and component-specific (blue line) fraction of variance explained by the top 5 principal components.

SI TABLES

1. **Table S1. Multivariate Rank Order of Diagnostic Metabolites and Their Correlation with Symptom Severity in Chronic Fatigue Syndrome. A. Males Top 25, B. Females Top 25, C. Males: Metabolites #26-61, D. Females: Metabolites #26-61.** Metabolites with variable importance in projection (VIP) scores ≥ 1.5 were considered significant. FDR = false discovery rate. KPS = Karnofsky performance score. Metabolites that were negatively correlated with KPS scores and elevated in CFS are indicated in red.
2. **Table S2. Metabolomics Quality Control: Work-Flow Reproducibility.**
3. **Table S3. Metabolomics Quality Control: Reproducibility of Metabolite Quantification.**
4. **Table S4. Principal Components Analysis. A. Males, B. Females.**

Table S1. The Top 25 Diagnostic Metabolites in Chronic Fatigue Syndrome. A. Males

No.	MRM Name	Pathway Name	VIP Score	P Value	FDR	Fold Change	Z Score	KPS* Correlation Spearman r	KPS* Correlation Spearman p
1	PC(16:0/16:0)	Phospholipid Metabolism	2.65	5.32E-05	0.023	0.76	-1.61	0.59	6.43E-05
2	GC(18:1/16:0)	Glycosphingolipid Metabolism	2.46	2.32E-04	0.025	0.59	-1.44	0.63	1.55E-05
3	Ceramide(d18:1/16:0)	Sphingolipid Metabolism	2.43	2.77E-04	0.025	0.69	-1.23	0.59	7.01E-05
4	THC 18:1/24:0	Glycosphingolipid Metabolism	2.39	3.74E-04	0.025	0.69	-1.22	0.55	2.12E-04
5	Ceramide(d18:1/24:2)	Sphingolipid Metabolism	2.51	1.61E-04	0.025	0.56	-1.32	0.54	3.10E-04
6	PI(38:4)	Phospholipid Metabolism	2.38	3.88E-04	0.025	0.78	-1.45	0.53	4.10E-04
7	DHC(18:1/16:0)	Glycosphingolipid Metabolism	2.38	4.04E-04	0.025	0.57	-1.26	0.53	4.72E-04
8	PA(16:0/16:0)	Phospholipid Metabolism	2.35	4.90E-04	0.026	0.75	-1.08	0.49	1.40E-03
9	1-Pyrroline-5-carboxylic acid	P5C, Arginine, Ornithine, Proline	2.26	8.38E-04	0.040	1.45	1.23	-0.53	4.91E-04
10	SM(d18:1/22:1 OH)	Sphingolipid Metabolism	2.20	1.24E-03	0.041	0.78	-1.31	0.53	4.01E-04
11	SM(d18:1/24:2 OH)	Sphingolipid Metabolism	2.21	1.15E-03	0.041	0.76	-1.19	0.46	2.84E-03
12	Ceramide(d18:1/16:1 OH)	Sphingolipid Metabolism	2.20	1.19E-03	0.041	0.71	-1.16	0.44	4.68E-03
13	SM(d18:1/22:0)	Sphingolipid Metabolism	2.20	1.22E-03	0.041	0.72	-0.99	0.43	5.29E-03
14	Ethanolamine	Phospholipid and Plasmalogen Metabolism	2.13	1.79E-03	0.055	0.81	-1.17	0.47	2.12E-03
15	FAD	Vitamin B2 (Riboflavin) Metabolism	2.05	2.83E-03	0.076	0.69	-0.85	0.49	1.29E-03
16	4-Hydroxyphenyllactic acid	Microbiome Metabolism	2.06	2.66E-03	0.076	0.73	-1.10	0.48	1.71E-03
17	Ceramide(d18:1/16:1)	Sphingolipid Metabolism	2.02	3.42E-03	0.085	0.78	-1.16	0.50	1.14E-03
18	Ceramide(d18:1/18:0)	Sphingolipid Metabolism	2.01	3.56E-03	0.085	0.61	-0.92	0.42	6.77E-03
19	SM(d18:1/16:0)	Sphingolipid Metabolism	1.91	5.86E-03	0.090	0.77	-1.01	0.54	3.65E-04
20	SM(d18:1/18:2 OH)	Sphingolipid Metabolism	1.92	5.55E-03	0.090	0.83	-1.02	0.44	4.85E-03
21	L-Serine	1-Carbon, Folate, Formate, Glycine, Serine	1.95	4.86E-03	0.090	1.27	1.25	-0.41	7.95E-03
22	Ceramide(d18:1/24:1)	Sphingolipid Metabolism	1.92	5.59E-03	0.090	0.71	-0.95	0.41	9.37E-03
23	Arginine	P5C, Arginine, Ornithine, Proline	1.91	5.71E-03	0.090	1.30	1.10	-0.40	1.10E-02
24	Methionine sulfoxide	SAM, SAH, Methionine, Cysteine, Glutathione	1.94	4.93E-03	0.090	1.47	0.94	-0.39	1.18E-02
25	Ceramide(d18:1/26:2)	Sphingolipid Metabolism	1.98	4.18E-03	0.090	0.66	-0.95	0.38	1.50E-02
					Decreased	0.72	-1.16	0.49	N = 21
					Increased	1.37	1.13	-0.43	N = 4

*KPS = Karnofsky performance scale
Metabolites that were negatively correlated with KPS scores and elevated in CFS are indicated in red.

Table S1. The Top 25 Diagnostic Metabolites in Chronic Fatigue Syndrome. B. Females

No.	MRM Name	Pathway Name	VIP Score	P Value	FDR	Fold Change	Z Score	KPS* Correlation Spearman r	KPS* Correlation Spearman p
1	Ceramide(d18:1/25:0)	Sphingolipid Metabolism	2.76	3.64E-05	0.009	0.55	-1.41	0.68	4.63E-07
2	THC 18:1/24:0	Glycosphingolipid Metabolism	2.72	4.83E-05	0.009	0.66	-1.48	0.56	6.49E-05
3	PC(16:0/16:0)	Phospholipid Metabolism	2.69	6.11E-05	0.009	0.79	-1.30	0.58	3.77E-05
4	Lathosterol	Cholesterol, Cortisol, Non-Gonadal Steroids	2.46	3.15E-04	0.028	0.67	-1.16	0.52	3.17E-04
5	Hydroxyproline	Vitamin C (Ascorbate) Metabolism/Collagen	2.44	3.73E-04	0.028	1.66	1.50	-0.50	5.62E-04
6	PI(16:0/16:0)	Phospholipid Metabolism	2.42	4.06E-04	0.028	0.40	-1.19	0.54	1.76E-04
7	Ceramide(d18:1/22:2)	Sphingolipid Metabolism	2.39	5.17E-04	0.031	0.59	-1.05	0.58	3.08E-05
8	Adenosine	Purine Metabolism	2.36	6.15E-04	0.032	0.49	-1.59	0.41	5.91E-03
9	Ceramide(d18:1/24:2)	Sphingolipid Metabolism	2.27	1.02E-03	0.044	0.55	-1.02	0.61	1.33E-05
10	THC 18:1/16:0	Glycosphingolipid Metabolism	2.26	1.10E-03	0.044	0.64	-1.22	0.49	7.85E-04
11	2-Octenoylcarnitine	Fatty Acid Oxidation and Synthesis	2.25	1.14E-03	0.044	0.55	-1.05	0.55	1.19E-04
12	GC(18:1/16:0)	Glycosphingolipid Metabolism	2.23	1.32E-03	0.046	0.66	-1.32	0.45	2.17E-03
13	Phenyllactic acid	Microbiome Metabolism	2.21	1.48E-03	0.048	0.65	-0.83	0.57	5.37E-05
14	Ceramide(d18:1/26:0)	Sphingolipid Metabolism	2.19	1.63E-03	0.048	0.66	-0.93	0.47	1.22E-03
15	Ceramide(d18:1/24:0)	Sphingolipid Metabolism	2.18	1.73E-03	0.048	0.65	-1.03	0.48	1.03E-03
16	DHC(18:1/16:0)	Glycosphingolipid Metabolism	2.16	1.95E-03	0.049	0.69	-1.23	0.44	2.88E-03
17	Ceramide(d18:1/26:2)	Sphingolipid Metabolism	2.16	1.96E-03	0.049	0.58	-0.88	0.54	1.33E-04
18	FAD	Vitamin B2 (Riboflavin) Metabolism	2.10	2.73E-03	0.064	0.73	-0.89	0.36	1.67E-02
19	1-Pyrroline-5-carboxylic acid	P5C, Arginine, Ornithine, Proline	2.08	2.96E-03	0.066	1.37	1.13	-0.35	2.05E-02
20	Ceramide(d18:1/16:0)	Sphingolipid Metabolism	2.03	3.86E-03	0.081	0.65	-0.90	0.47	1.21E-03
21	SM(d18:1/22:2)	Sphingolipid Metabolism	2.01	4.13E-03	0.081	0.74	-0.92	0.28	6.52E-02
22	Adenosine monophosphate	Purine Metabolism	2.01	4.21E-03	0.081	0.82	-0.82	0.40	7.16E-03
23	PC(18:1/22:5)	Phospholipid Metabolism	1.99	4.64E-03	0.085	1.33	0.87	-0.34	2.41E-02
24	PI(38:3)	Phospholipid Metabolism	1.97	5.07E-03	0.089	0.76	-0.93	0.41	5.24E-03
25	PC(22:6/P-18:0)	Plasmalogen Metabolism	1.96	5.37E-03	0.090	1.52	1.29	-0.42	4.08E-03
					Decreased	0.64	-1.10	0.49	N = 21
					Increased	1.47	1.20	-0.40	N = 4

*KPS = Karnofsky performance scale

Metabolites that were negatively correlated with KPS scores and were elevated in CFS are indicated in red.

Table S1. Diagnostic Metabolites #26-61 in Chronic Fatigue Syndrome. C. Males

No.	MRM Name	Pathway Name	VIP Score	P Value	FDR	Fold Change	Z Score	KPS* Correlation Spearman r	KPS* Correlation Spearman p
26	Ceramide(d18:1/25:0)	Sphingolipid Metabolism	1.92	0.005	0.090	0.689	-0.803	0.362	0.022
27	Ceramide(d18:1/22:2)	Sphingolipid Metabolism	1.95	0.005	0.090	0.710	-0.863	0.358	0.023
28	Ceramide(d18:1/22:1)	Sphingolipid Metabolism	1.93	0.005	0.090	0.685	-0.946	0.351	0.026
29	Behenic acid	Very Long Chain Fatty Acid Oxidation	1.84	0.008	0.124	0.652	-0.718	0.279	0.081
30	Hydroxyisocaproic acid	Branch Chain Amino Acid Metabolism	1.80	0.010	0.139	0.756	-0.920	0.339	0.032
31	Uric acid	Purine Metabolism	1.79	0.010	0.142	0.886	-0.872	0.398	0.011
32	Pyroglutamic acid	GABA, Glutamate Metabolism	1.75	0.012	0.146	0.839	-1.432	0.487	0.001
33	SM(d18:1/24:0)	Sphingolipid Metabolism	1.75	0.012	0.146	0.801	-0.829	0.369	0.019
34	Lathosterol	Cholesterol, Cortisol, Non-Gonadal Steroid	1.78	0.011	0.146	0.825	-1.051	0.317	0.046
35	PC(16:0/20:4)	Phospholipid Metabolism	1.77	0.011	0.146	0.828	-1.039	0.295	0.064
36	PC(18:1/22:6)	Phospholipid Metabolism	1.76	0.012	0.146	1.283	0.924	-0.261	0.104
37	SM(d18:1/22:1)	Sphingolipid Metabolism	1.74	0.013	0.146	0.795	-0.918	0.408	0.009
38	Ceramide(d18:1/22:0)	Sphingolipid Metabolism	1.72	0.014	0.159	0.743	-0.785	0.386	0.014
39	SM(d18:1/16:0 OH)	Sphingolipid Metabolism	1.71	0.015	0.165	0.837	-1.012	0.415	0.008
40	Ceramide(d18:1/24:0)	Sphingolipid Metabolism	1.69	0.016	0.169	0.788	-0.822	0.403	0.010
41	SM(d18:1/20:2 OH)	Sphingolipid Metabolism	1.69	0.016	0.170	0.826	-0.974	0.299	0.061
42	PC(18:1/18:1)	Phospholipid Metabolism	1.67	0.017	0.174	0.826	-0.901	0.319	0.045
43	Ceramide(d18:1/16:2 OH)	Sphingolipid Metabolism	1.66	0.018	0.178	0.780	-0.886	0.377	0.016
44	PC(20:5/P-16:0)	Phospholipid Metabolism	1.65	0.019	0.183	1.444	0.902	-0.273	0.088
45	PI(38:3)	Phospholipid Metabolism	1.62	0.021	0.192	0.847	-0.763	0.374	0.017
46	L-Threonine	Amino Acid Metabolism	1.62	0.021	0.192	1.188	0.871	-0.365	0.020
47	2-Methylcitric acid	Isoleucine, Valine, Threonine, or Methionine	1.63	0.021	0.192	0.789	-1.177	0.362	0.022
48	SM(d18:1/22:0 OH)	Sphingolipid Metabolism	1.61	0.022	0.192	0.847	-0.756	0.341	0.032
49	24,25-Epoxycholesterol	Cholesterol, Cortisol, Non-Gonadal Steroid	1.62	0.022	0.192	0.782	-0.858	0.272	0.089
50	Cholesterol	Cholesterol, Cortisol, Non-Gonadal Steroid	1.60	0.023	0.200	0.882	-0.750	0.419	0.007
51	SM(d18:1/18:0)	Sphingolipid Metabolism	1.59	0.024	0.205	0.816	-0.681	0.399	0.011
52	Ceramide(d18:1/24:0 OH)	Sphingolipid Metabolism	1.56	0.026	0.212	0.708	-0.685	0.336	0.034
53	SM(d18:1/22:2)	Sphingolipid Metabolism	1.57	0.026	0.212	0.776	-0.635	0.285	0.074
54	2-Hydroxy-3-methylbutyrate	Branch Chain Amino Acid Metabolism	1.56	0.027	0.212	0.761	-0.710	0.225	0.162
55	Ceramide(d18:1/16:0 OH)	Sphingolipid Metabolism	1.55	0.028	0.214	0.750	-0.663	0.370	0.019
56	Deoxyguanosine	Purine Metabolism	1.55	0.028	0.214	0.769	-0.755	0.257	0.110
57	Gamma-Aminobutyric acid	GABA, Glutamate Metabolism	1.55	0.028	0.214	1.221	0.706	-0.188	0.244
58	Tiglylcarnitine	Branch Chain Amino Acid Metabolism	1.51	0.033	0.230	0.750	-0.725	0.435	0.005
59	SM(d18:1/16:1 OH)	Sphingolipid Metabolism	1.51	0.032	0.230	0.867	-0.926	0.417	0.007
60	Ceramide(d18:1/18:1 OH)	Sphingolipid Metabolism	1.52	0.031	0.230	0.814	-0.795	0.257	0.109
61	SM(d18:1/25:0)	Sphingolipid Metabolism	1.51	0.032	0.230	0.827	-0.625	0.208	0.197
					Decreased	0.789	-0.852	0.348	N = 32
					Increased	1.284	0.851	-0.272	N = 4

*KPS = Karnofsky performance scale

Metabolites that were negatively correlated with KPS scores and were elevated in CFS are indicated in red.

Table S1. Diagnostic Metabolites #26-61 in Chronic Fatigue Syndrome. D. Females

No.	MRM Name	Pathway Name	VIP Score	P Value	FDR	Fold Change	Z Score	KPS* Correlation Spearman r	KPS* Correlation Spearman p
26	PC(36:0)	Phospholipid Metabolism	1.93	0.006	0.103	1.274	1.142	-0.375	0.012
27	Chenodeoxycholic acid	Bile Salt Metabolism	1.90	0.007	0.107	0.504	-0.828	0.403	0.007
28	Ceramide(d18:1/20:0)	Sphingolipid Metabolism	1.90	0.007	0.107	0.654	-0.853	0.437	0.003
29	PC(18:1/22:6)	Phospholipid Metabolism	1.88	0.008	0.113	1.373	1.151	-0.392	0.009
30	Ceramide(d18:1/22:1 OH)	Sphingolipid Metabolism	1.86	0.009	0.116	0.637	-0.741	0.480	0.001
31	Ceramide(d18:1/18:2 OH)	Sphingolipid Metabolism	1.86	0.009	0.116	0.662	-0.785	0.450	0.002
32	Ceramide(d18:1/22:0)	Sphingolipid Metabolism	1.83	0.010	0.129	0.667	-0.801	0.445	0.002
33	Ceramide(d18:1/18:0)	Sphingolipid Metabolism	1.82	0.010	0.129	0.567	-0.730	0.415	0.005
34	Ceramide(d18:1/16:1 OH)	Sphingolipid Metabolism	1.82	0.010	0.129	0.704	-0.809	0.429	0.004
35	Ceramide(d18:1/24:2 OH)	Sphingolipid Metabolism	1.79	0.012	0.136	0.644	-0.766	0.457	0.002
36	SM(d18:1/16:0)	Sphingolipid Metabolism	1.79	0.012	0.136	0.748	-0.890	0.274	0.072
37	Ceramide(d18:1/24:1)	Sphingolipid Metabolism	1.77	0.013	0.144	0.685	-0.813	0.500	0.001
38	PI(34:1)	Phospholipid Metabolism	1.75	0.014	0.152	0.765	-0.792	0.362	0.016
39	PI(36:0)	Phospholipid Metabolism	1.72	0.016	0.171	0.742	-0.781	0.369	0.014
40	SM(d18:1/20:1)	Sphingolipid Metabolism	1.71	0.016	0.171	0.775	-0.843	0.415	0.005
41	Adipoylcarnitine	Fatty Acid Oxidation and Synthesis	1.71	0.017	0.172	1.401	1.338	-0.360	0.016
42	2-Arachidonylglycerol	Endocannabinoid Metabolism	1.69	0.018	0.174	0.681	-0.749	0.428	0.004
43	THC 18:1/18:0	Glycosphingolipid Metabolism	1.69	0.018	0.174	0.756	-0.906	0.346	0.021
44	Ceramide(d18:1/22:1)	Sphingolipid Metabolism	1.68	0.019	0.180	0.680	-0.712	0.414	0.005
45	PI(34:0)	Phospholipid Metabolism	1.66	0.020	0.183	0.757	-0.714	0.380	0.011
46	Ceramide(d18:1/26:1 OH)	Sphingolipid Metabolism	1.66	0.020	0.183	0.655	-0.717	0.469	0.001
47	PI(38:4)	Phospholipid Metabolism	1.65	0.021	0.185	0.812	-0.665	0.351	0.020
48	Hydroxyisocaproic acid	Branch chain amino acids	1.64	0.022	0.193	0.720	-0.618	0.381	0.011
49	PC(16:0/22:6)	Phospholipid Metabolism	1.61	0.025	0.211	1.249	0.711	-0.306	0.043
50	PC(30:0)	Phospholipid Metabolism	1.60	0.025	0.211	0.840	-0.729	0.358	0.017
51	Cobalamin	Vitamin B12 (Cobalamin) Metabolism	1.60	0.026	0.211	0.803	-1.062	0.157	0.308
52	Ceramide(d18:1/20:1 OH)	Sphingolipid Metabolism	1.59	0.026	0.213	0.659	-0.603	0.447	0.002
53	dAMP	Purine Metabolism	1.59	0.027	0.214	0.902	-0.865	0.326	0.031
54	Arginine	P5C, Arginine, Ornithine, Proline	1.56	0.030	0.233	1.206	0.821	-0.131	0.397
55	PC(38:5)	Phospholipid Metabolism	1.54	0.031	0.233	1.229	0.710	-0.296	0.051
56	Gluconic acid	Microbiome Metabolism	1.54	0.032	0.233	1.261	0.694	-0.257	0.092
57	PG(32:2)	Phospholipid Metabolism	1.54	0.032	0.233	0.492	-0.565	0.364	0.015
58	Vitamin K2	Microbiome Metabolism	1.53	0.033	0.233	1.166	0.683	-0.223	0.145
59	PC(16:0/18:2)	Phospholipid Metabolism	1.53	0.033	0.233	0.922	-0.599	0.344	0.022
60	Glucosamine 6-phosphate	Amino sugars	1.52	0.034	0.233	1.207	0.669	-0.285	0.060
61	PI(36:1)	Phospholipid Metabolism	1.52	0.034	0.233	0.773	-0.691	0.329	0.029
					Decreased	0.686	-0.737	0.376	N = 27
					Increased	1.263	0.792	-0.263	N = 9

*KPS = Karnofsky performance scale
Metabolites that were negatively correlated with KPS scores and were elevated in CFS are indicated in red.

Table S2. Metabolomics Quality Control: Work-Flow Reproducibility.

Daily QC Metabolites	Within Day Pearson r	Within + Between Day Pearson r	Within Day Median RSD	Within + Between Day Median RSD
27 Stable Isotope (^{13}C,^{15}N,^{2}H)-Labeled Internal Standards	0.999	0.987	6.2%	9.1%
50 Endogenous Metabolites in Standard Pooled Human Plasma	0.998	0.981	8.4%	10.7%

Table S3. Metabolomics Quality Control: Reproducibility of Metabolite Quantification.

Representative Plasma Samples	Within Day Pearson r	Within + Between Day Pearson r	Within Day Median RSD	Within + Between Day Median RSD
458 Metabolites in Sample 1	0.998	0.983	10.2%	12.1%
458 Metabolites in Sample 2	0.997	0.981	11.3%	12.5%

Table S4A. Principal Components Analysis, Males. Top 10 Metabolites.

No.	PC1 Metabolite	PC1-12.4%	PC2 Metabolite	PC2-8.2%
1	Ceramide(d18:1/18:0)	0.11255	L-Kynurenine	0.12502
2	Ceramide(d18:1/16:0)	0.10299	Methylcysteine	0.11606
3	BMP(18:1/16:0)	0.099692	L-Lysine	0.11594
4	Ceramide(d18:1/24:0)	0.099161	Ureidopropionic acid	0.11379
5	SM(d18:1/20:2)	0.099053	L-Tyrosine	0.1135
6	Ceramide(d18:1/16:1 OH)	0.09877	1-Methylhistidine	0.10692
7	Ceramide(d18:1/24:2)	0.098766	Ornithine	0.10628
8	Ceramide(d18:1/20:1)	0.098707	L-Glutamine	0.10504
9	Ceramide(d18:1/22:0)	0.098347	Imidazoleacetic acid	0.10467
10	Ceramide(d18:1/24:0 OH)	0.097983	Kynurenic acid	0.089947

Table S4B. Principal Components Analysis, Females. Top 10 Metabolites.

No.	PC1 Metabolite	PC1-12%	PC2 Metabolite	PC2-9.9%
1	N-Acetyl-L-aspartic acid	0.071768	Oleic acid	0.09896
2	Arachidonyl carnitine	0.069874	Linoleic acid	0.098395
3	Hexose Monophosphate Pool	0.058809	12-HETE	0.090984
4	3, 5-Tetradecadiencarnitine	0.058589	L-Acetylcarnitine	0.090299
5	Glycine	0.057178	Glyoxylic acid	0.088276
6	Oleoylcarnitine	0.05567	3-Hydroxyhexadecenoylcarnitine	0.080763
7	2-Aminoisobutyric acid	0.055047	Arachidonic Acid	0.076768
8	N-acetylserine	0.053443	PS(36:2)	0.076663
9	O-acetylserine	0.052228	PS(18:0/20:4)	0.076464
10	3-Hydroxy-cis-5-tetradecenoylcarnitine	0.052165	4-Hydroxybenzoic acid	0.075434

Figure S1.

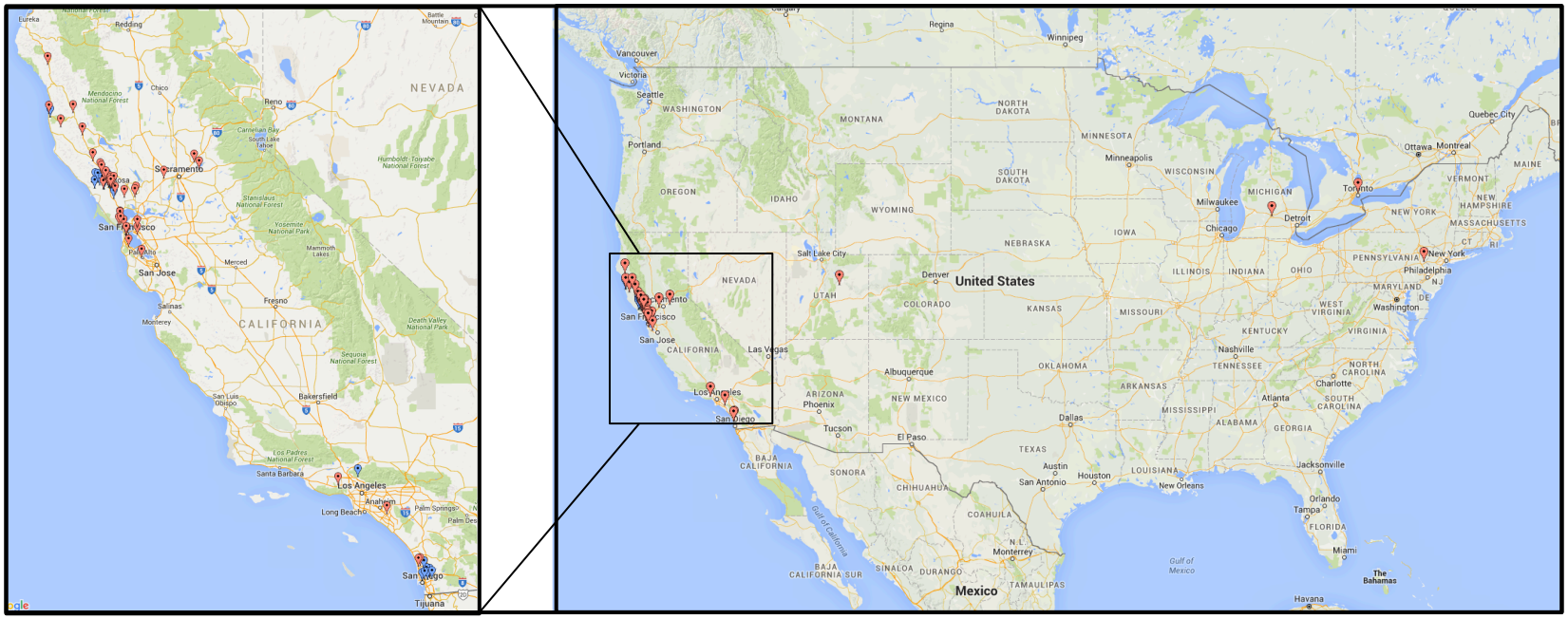
NEVADA
CALIFORNIA
Sacramento
San Jose
Fresno
Bakersfield
Los Angeles
San Diego
Tijuana
Las Vegas
Salt Lake City
Denver
United States
Albuquerque
Phoenix
Tucson
El Paso
Dallas
Houston
San Antonio
Austin
Chicago
Minneapolis
Detroit
Toronto
Ottawa
Montreal
Quebec City
New York
Philadelphia
Washington
Atlanta
Miami
Jacksonville
New Orleans
Nashville
Charlotte
Portland
Seattle
Vancouver
Winnipeg
Regina
Milwaukee
Mexico
Monterrey
Havana
The Bahamas
Gulf of Mexico
Gulf of California

Figure S2A. Males

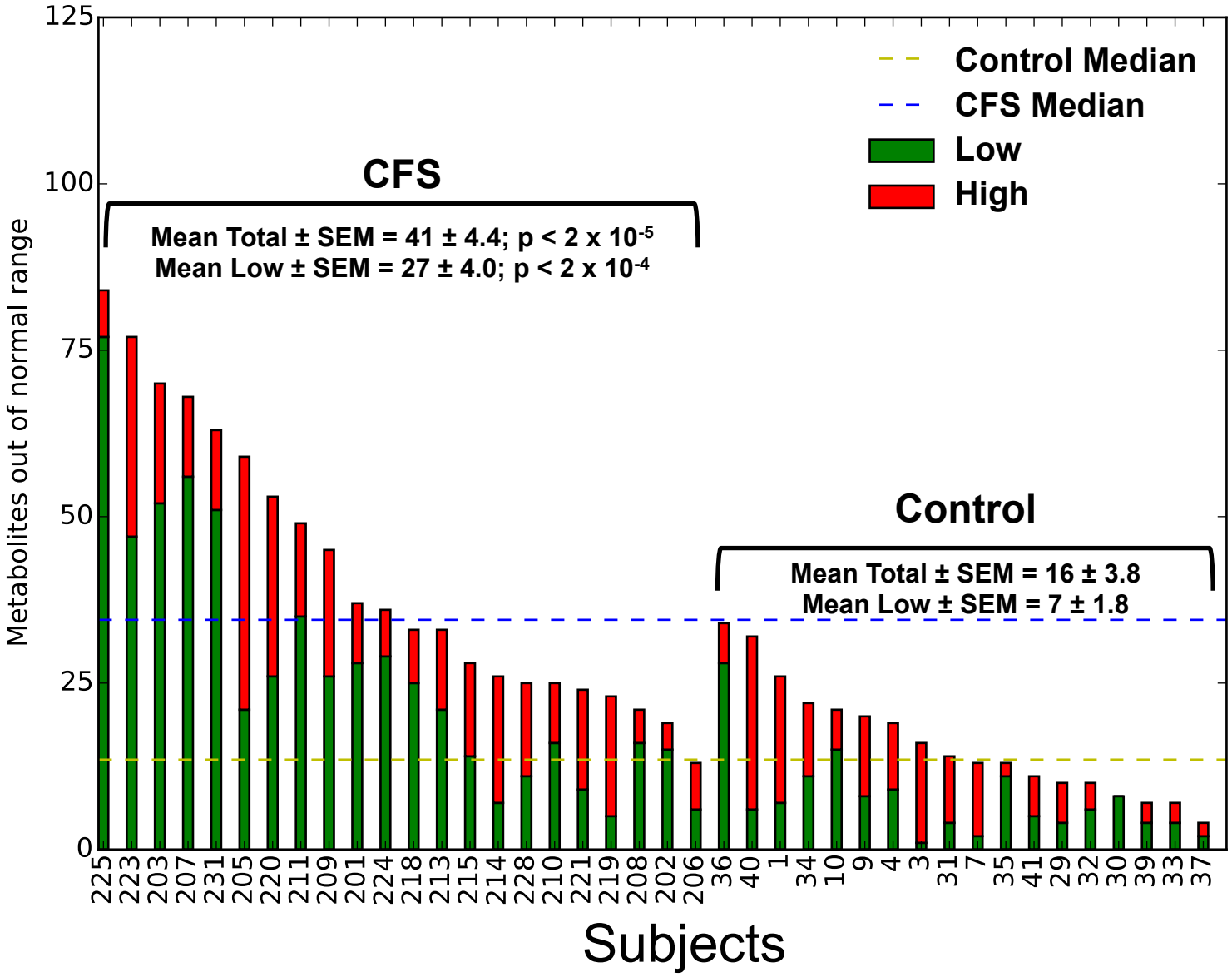

Figure S2B. Females.

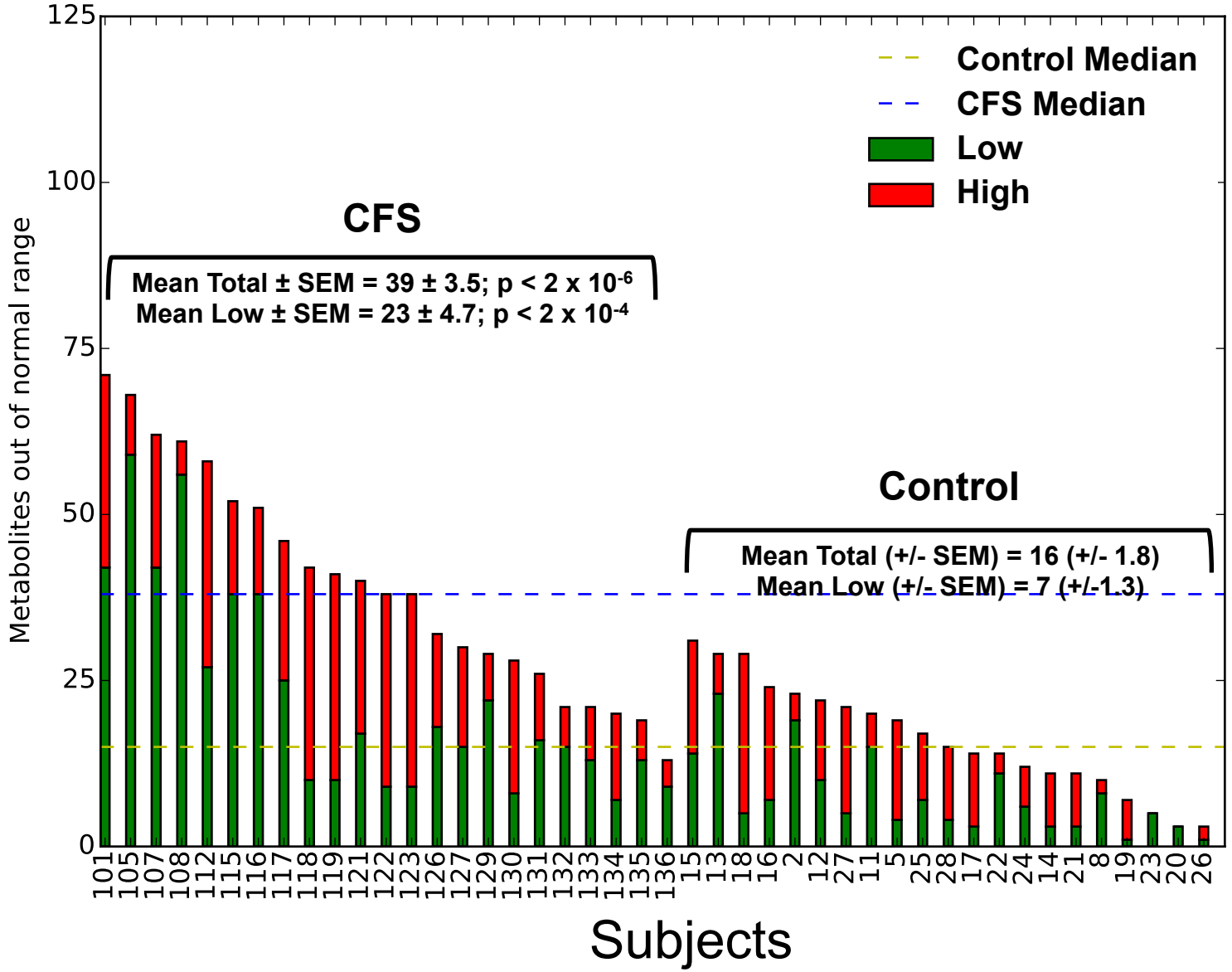

Figure S3.

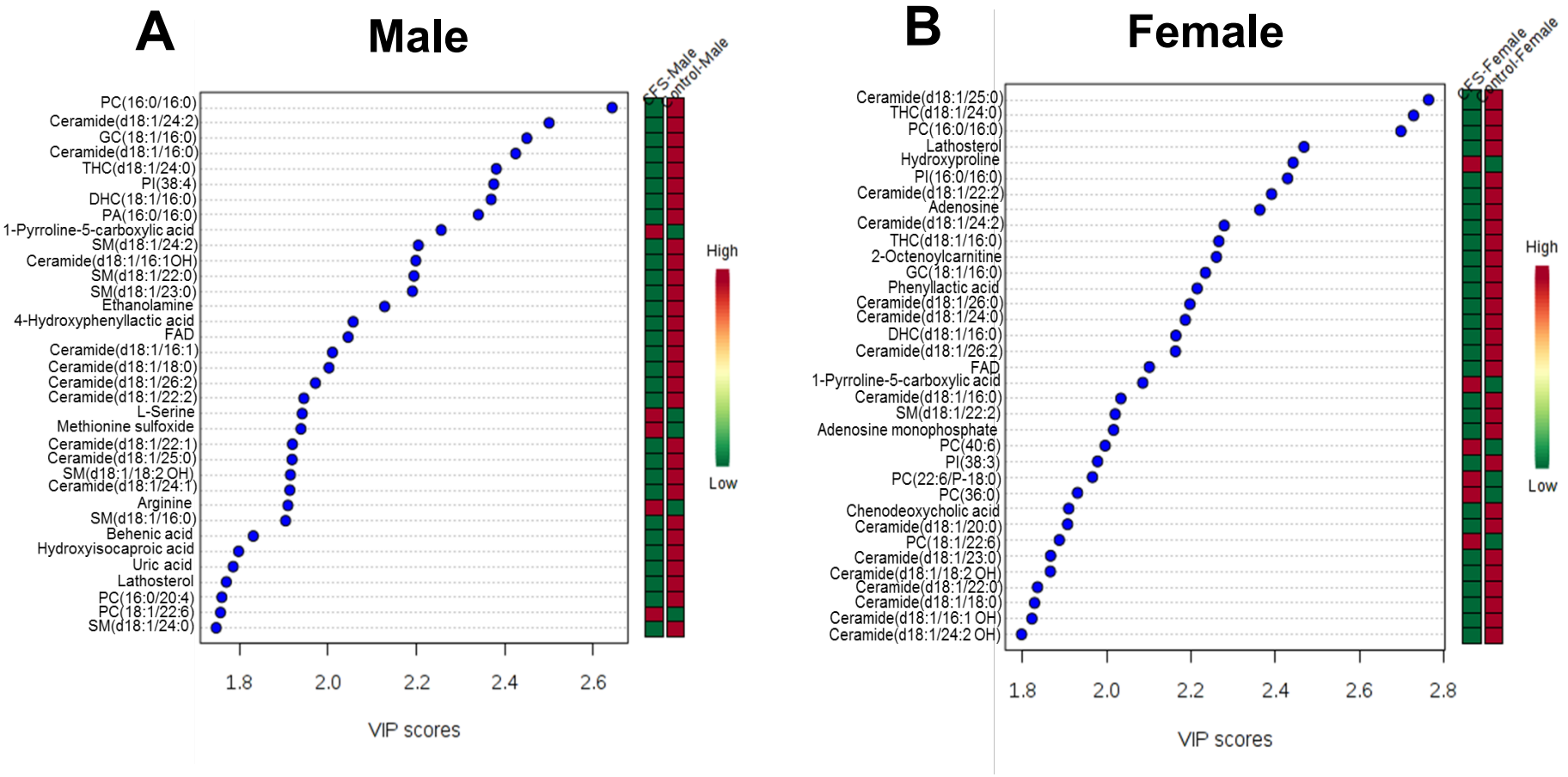
A
Male
PC(16:0/16:0)
Ceramide(d18:1/24:2)
GC(18:1/16:0)
Ceramide(d18:1/16:0)
THC(d18:1/24:0)
PI(38:4)
DHC(18:1/16:0)
PA(16:0/16:0)
1-Pyrroline-5-carboxylic acid
SM(d18:1/24:2)
Ceramide(d18:1/16:1OH)
SM(d18:1/22:0)
SM(d18:1/23:0)
Ethanolamine
4-Hydroxyphenyllactic acid
FAD
Ceramide(d18:1/16:1)
Ceramide(d18:1/18:0)
Ceramide(d18:1/26:2)
Ceramide(d18:1/22:2)
L-Serine
Methionine sulfoxide
Ceramide(d18:1/22:1)
Ceramide(d18:1/25:0)
SM(d18:1/18:2 OH)
Ceramide(d18:1/24:1)
Arginine
SM(d18:1/16:0)
Behenic acid
Hydroxyisocaproic acid
Uric acid
Lathosterol
PC(16:0/20:4)
PC(18:1/22:6)
SM(d18:1/24:0)
1.8
2.0
2.2
2.4
2.6
VIP scores
CFS-Male
Control-Male
High
Low
B
Female
Ceramide(d18:1/25:0)
THC(d18:1/24:0)
PC(16:0/16:0)
Lathosterol
Hydroxyproline
PI(16:0/16:0)
Ceramide(d18:1/22:2)
Adenosine
Ceramide(d18:1/24:2)
THC(d18:1/16:0)
2-Octenoylcarnitine
GC(18:1/16:0)
Phenyllactic acid
Ceramide(d18:1/26:0)
Ceramide(d18:1/24:0)
DHC(d18:1/16:0)
Ceramide(d18:1/26:2)
FAD
1-Pyrroline-5-carboxylic acid
Ceramide(d18:1/16:0)
SM(d18:1/22:2)
Adenosine monophosphate
PC(40:6)
PI(38:3)
PC(22:6/P-18:0)
PC(36:0)
Chenodeoxycholic acid
Ceramide(d18:1/20:0)
PC(18:1/22:6)
Ceramide(d18:1/23:0)
Ceramide(d18:1/18:2 OH)
Ceramide(d18:1/22:0)
Ceramide(d18:1/18:0)
Ceramide(d18:1/16:1 OH)
Ceramide(d18:1/24:2 OH)
1.8
2.0
2.2
2.4
2.6
2.8
VIP scores
CFS-Female
Control-Female
High
Low

Figure S4.

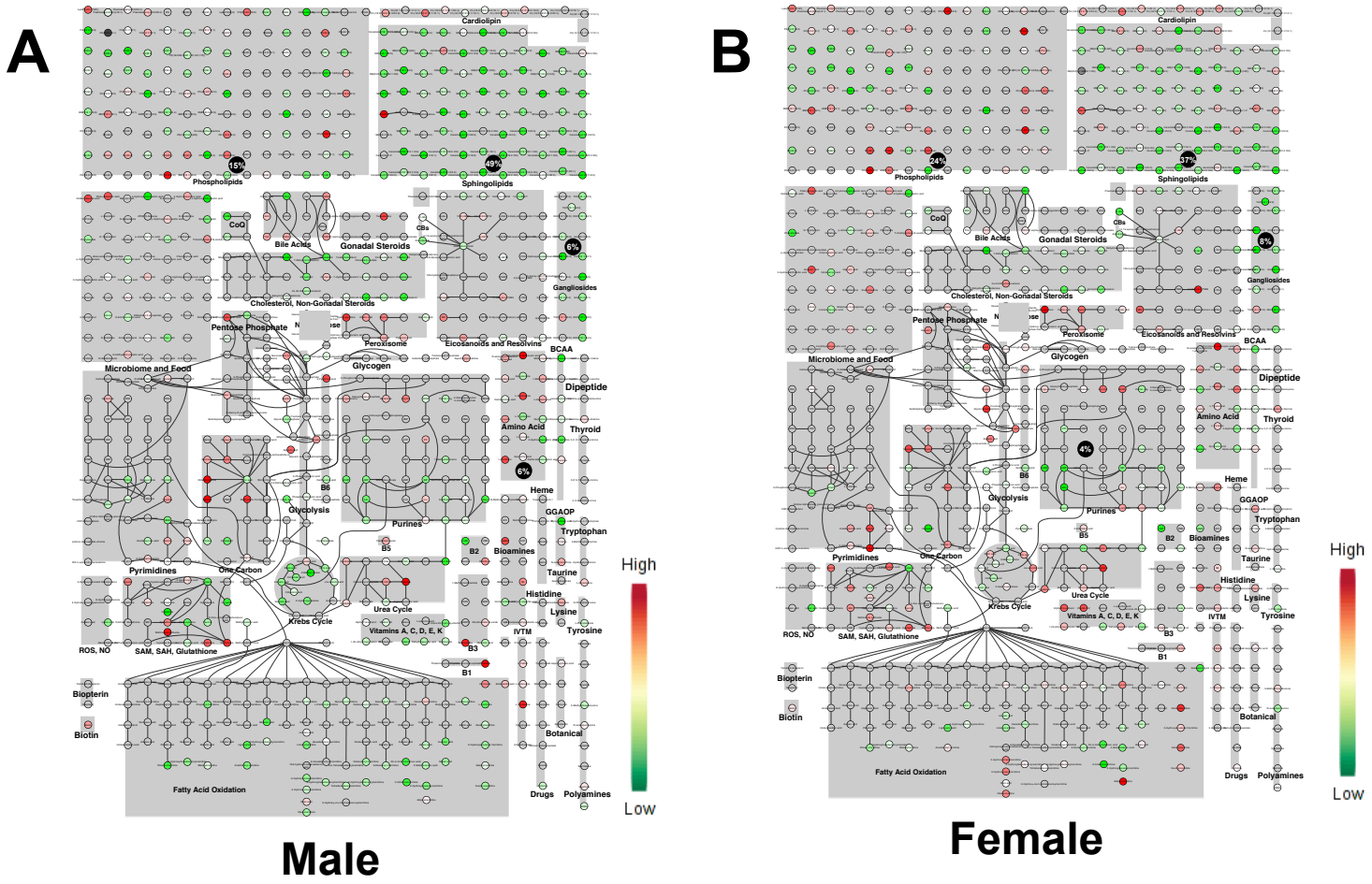
A
B
Cardiolipin
Phospholipids
Sphingolipids
CoQ
Bile Acids
Gonadal Steroids
GBs
Gangliosides
Cholesterol, Non-Gonadal Steroids
Pentose Phosphate
Peroxisome
Eicosanoids and Resolvins
BCAA
Glycogen
Microbiome and Food
Dipeptide
Amino Acid
Thyroid
Heme
GGAOP
Tryptophan
Glycolysis
Purines
B6
B5
B2
Bioamines
Taurine
Pyrimidines
One Carbon
Histidine
Lysine
Urea Cycle
Krebs Cycle
Vitamins A, C, D, E, K
IVTM
Tyrosine
B3
ROS, NO
SAM, SAH, Glutathione
B1
Biopterin
Biotin
Botanical
Fatty Acid Oxidation
Drugs
Polyamines
High
Low
Male
Female

Figure S5. Males.

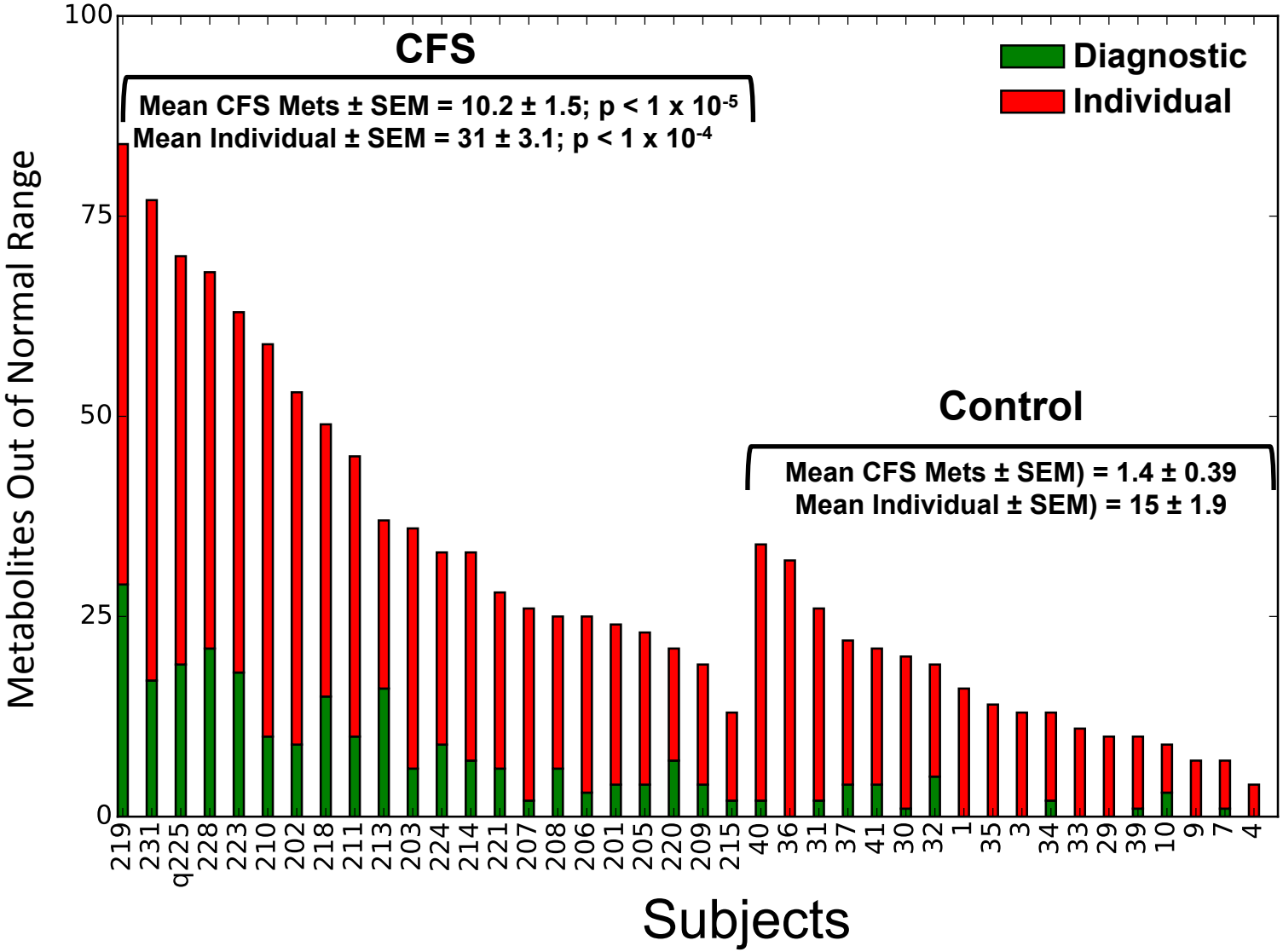

Figure S6.

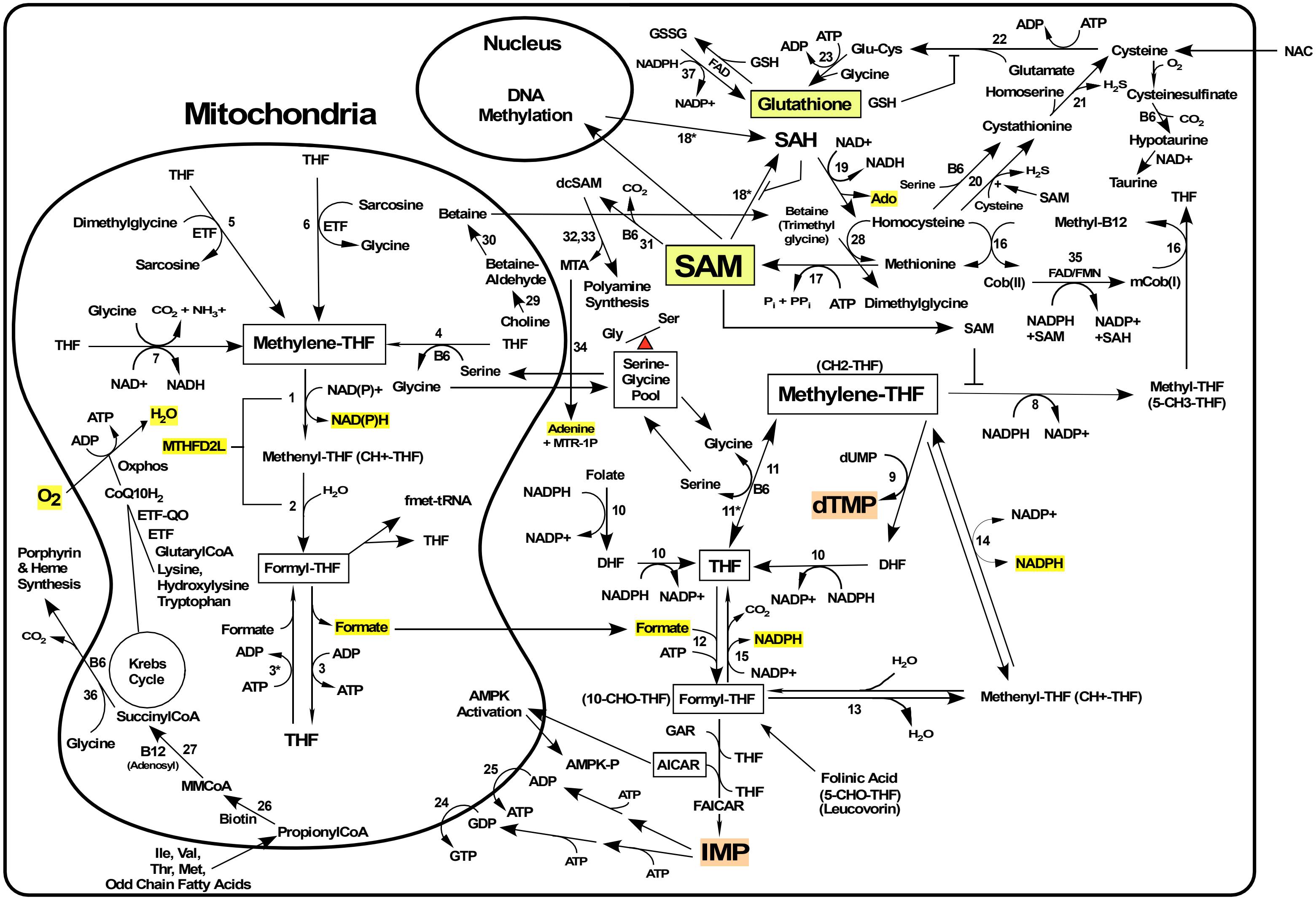

Mitochondria
Nucleus
DNA Methylation
Glutathione
SAM
SAH
Methylene-THF
Methenyl-THF (CH+-THF)
Formyl-THF
THF
Serine-Glycine Pool
(CH2-THF)
Methyl-THF (5-CH3-THF)
dTMP
IMP
AICAR
Formate
MTHFD2L
NAD(P)H
Adenine + MTR-1P
Ado
Krebs Cycle
Porphyrin & Heme Synthesis
AMPK Activation
AMPK-P
Folinic Acid (5-CHO-THF) (Leucovorin)
(10-CHO-THF)
Cysteine
NAC
Homocysteine
Methionine
Cystathionine
Taurine
Hypotaurine
Cysteinesulfinate
Betaine
Choline
Sarcosine
Dimethylglycine
Glycine
Serine
Polyamine Synthesis
dcSAM
MTA
Oxphos
CoQ10H2
ETF-QO
GlutarylCoA
Lysine, Hydroxylysine Tryptophan
SuccinylCoA
MMCoA
PropionylCoA
Ile, Val, Thr, Met, Odd Chain Fatty Acids
Methyl-B12
mCob(I)
Cob(II)
fmet-tRNA

Figure S7A. Males

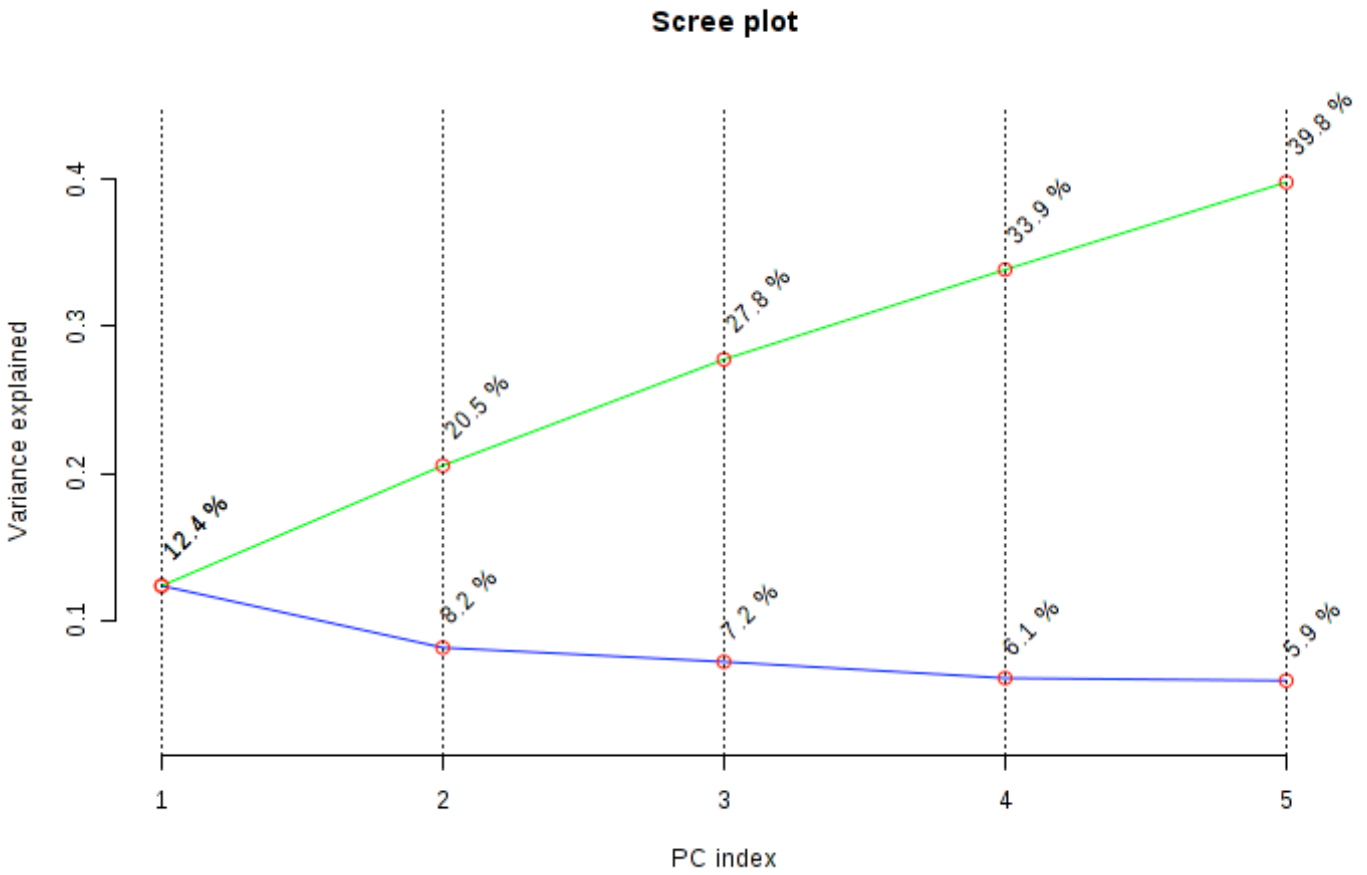

Figure S7B. Females